Accepted Manuscript

Pyrazinyl ureas revisited: 1-(3-(Benzyloxy)pyrazin-2-yl)-3-(3,4-dichlorophenyl)urea, a new blocker of Aβ-induced mPTP opening for Alzheimer's disease

Ahmed Elkamhawy, Jung-eun Park, Ahmed H.E. Hassan, Ae Nim Pae, Jiyoun Lee, Sora Paik, Beoung-Geon Park, Eun Joo Roh

PII: S0223-5234(18)30633-0

DOI: 10.1016/j.ejmech.2018.07.068

Reference: EJMECH 10603

To appear in: *European Journal of Medicinal Chemistry*

Received Date: 4 April 2018

Revised Date: 27 July 2018

Accepted Date: 29 July 2018

Please cite this article as: A. Elkamhawy, J.-e. Park, A.H.E. Hassan, A.N. Pae, J. Lee, S. Paik, B.-G. Park, E.J. Roh, Pyrazinyl ureas revisited: 1-(3-(Benzyloxy)pyrazin-2-yl)-3-(3,4-dichlorophenyl)urea, a new blocker of Aβ-induced mPTP opening for Alzheimer's disease, *European Journal of Medicinal Chemistry* (2018), doi: 10.1016/j.ejmech.2018.07.068.

Graphical Abstract:

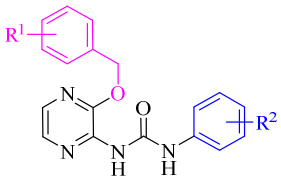

6 derivatives

	Increased g/r ratio (%)
I : R^1 = H, R^2 = 2-F	132
II : R^1 = H, R^2 = 3-F	111
III : R^1 = 3-F, R^2 = H	69
IV : R^1 = 3-F, R^2 = 3-F	98
V : R^1 = 3-F, R^2 = 3-Cl, 4-Cl	101
VI : R^1 = 3-F, R^2 = 4-Me	96

All reported pyrazinyl ureas (Non active)

Current study

Structural modifications

Various substitution patterns on the benzyloxy moiety

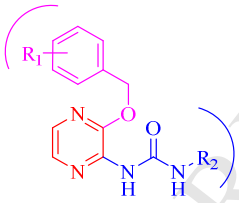

Comprehensive substituion investigation iclude: alkyl, cycloalkyl, aromatic, 1-methylpiperazinyl, piperazinyl moities

Pyrazinyl urea scaffold reassessment against mPTP opening activity

1-28

Newly synthesized active pyrazinyl ureas

Pyrazinyl ureas revisited: 1-(3-(Benzyloxy)pyrazin-2-yl)-3-(3,4-dichlorophenyl)urea, a new blocker of Aβ-induced mPTP opening for Alzheimer's disease

Ahmed Elkamhawy[a,b,1,*], Jung-eun Park[a,c,1], Ahmed H. E. Hassan[d], Ae Nim Pae[e,f], Jiyoun Lee[g], Sora Paik[a,h], Beoung-Geon Park[e], Eun Joo Roh[a,f,*]

[a] *Chemical Kinomics Research Center, Korea Institute of Science and Technology (KIST), Seoul 02792, Republic of Korea*

[b] *Department of Pharmaceutical Organic Chemistry, Faculty of Pharmacy, Mansoura University, Mansoura 35516, Egypt*

[c] *Department of Chemistry, Sogang University, Seoul 04107, Republic of Korea*

[d] *Department of Medicinal Chemistry, Faculty of Pharmacy, Mansoura University, Mansoura 35516, Egypt*

[e] *Convergence Research Center for Diagnosis, Treatment and Care System of Dementia, Korea Institute of Science and Technology (KIST), Seoul 02792, Republic of Korea*

[f] *Division of Bio-Medical Science & Technology, KIST School, Korea University of Science and Technology, Seoul 02792, Republic of Korea*

[g] *Department of Global Medical Science, Sungshin Women's University, Seoul 142-732, Republic of Korea*

[h] *Department of Fundamental Pharmaceutical Sciences, College of Pharmacy, Kyung Hee University, Seoul, 02447, Republic of Korea*

[*] Corresponding authors:

Ahmed Elkamhawy: a_elkamhawy@mans.edu.eg ; a.elkamhawy@gmail.com

Eun Joo Roh: r8636@kist.re.kr

[1] Both authors contributed equally to this work

Abstract

Herein, we report synthesis and evaluation of new twenty-eight pyrazinyl ureas against β amyloid (Aβ)-induced opening of mitochondrial permeability transition pore (mPTP) using JC-1 assay which measures the change of mitochondrial membrane potential ($\Delta\Psi m$). The neuroprotective effect of seventeen compounds against Aβ-induced mPTP opening was superior to that of the standard Cyclosporin A (CsA). Among them, 1-(3-(benzyloxy)pyrazin-2-yl)-3-(3,4-dichlorophenyl)urea (**5**) effectively maintained mitochondrial function and cell viabilities on ATP assay and MTT assay. Also, hERG channel assay presented safe cardiotoxicity profile for compound **5**. In addition, using CDocker algorithm, a molecular docking model presented a plausible explanation for the elicited differences in efficiencies of the synthesized compounds to reduce the green to red fluorescence as indication of mPTP closure. Hence, this report presents compound **5** as the most promising pyrazinyl urea-based mPTP blocker up to date.

Keywords: β-amyloid peptide (Aβ); Mitochondrial permeability transition pore (mPTP); Aβ-induced neurotoxicity; Alzheimer's disease (AD); urea; Cyclophilin D

1. Introduction

As the most common cause of dementia, Alzheimer's disease (AD) comes to the fore with 60−70% of cases [1, 2]. The excessive production of β-amyloid peptide (Aβ) and its extracellular deposition is a significant key factor associated with Alzheimer's disease etiology [3]. Recent reports indicate that mitochondrial permeability transition pore (mPTP) is a confirmed target for the soluble Aβ oligomers since it plays a key role in mitochondrial dysfunction induced by Aβ toxicity [4-6]. The multiprotein complex (mPTP) could be formed in mitochondria under certain pathological conditions including traumatic membrane injury, oxidative stress, ischemia, and stroke. The recent acceptable model of mPTP shows that its core consists of F_0/F_1 ATPase dimers in direct interaction with the regulatory CypD in the mitochondrial matrix [7]. Accumulation of the soluble Aβ oligomers results in excessive calcium entry into cytosol with consequent uncontrolled mPTP opening followed by inhibition of mitochondrial ATP production, mitochondrial swelling and outer membrane rupture. In fact, CypD was reported to be the mPTP component that responds to various stimuli and initiates opening of mPTP [8]. Thus, development of novel mPTP blockers targeting CypD as a main component of the pore could serve as a promising approach for treatment of Alzheimer's disease [5, 9, 10]. However, some peptidic compounds as cyclosporin A (CsA) and its analog *N*-methyl-4-isoleucine cyclosporin (NIM811) which have been identified as mPTP inhibitors showed no promising therapy due to hurdles of peptide delivery to the brain, reports of efforts to develop mPTP opening modulators are limited in literature (Fig. 1) [11-15]. To the best of our knowledge, the therapeutic small molecule blocker of mPTP has not been realized yet.

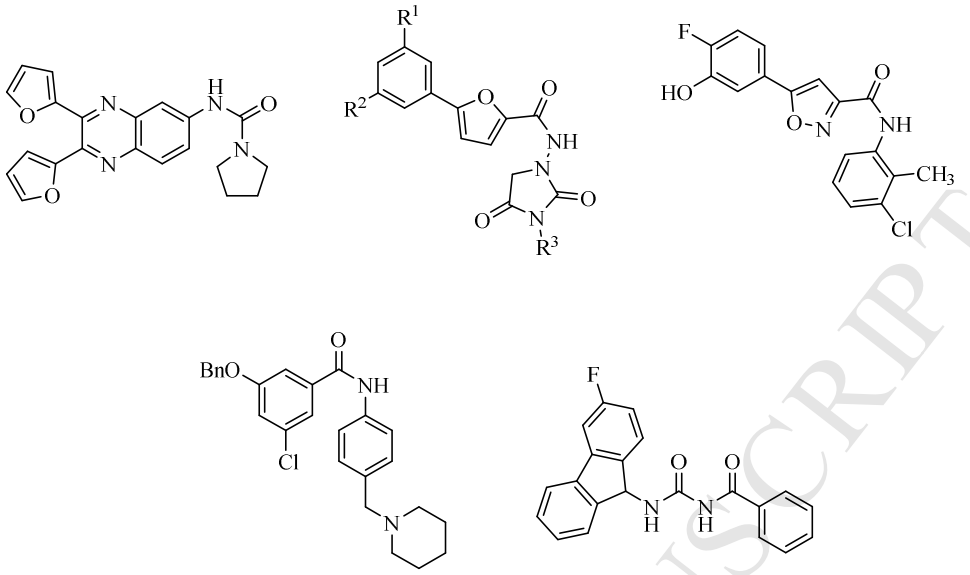

Fig. 1. Previously reported chemical entities with potential mPTP inhibition activity

This encouraged our institute to launch a discovery project towards identification of promising mPTP modulators. As a result, different chemical scaffolds-based small molecules have been reported as potential mPTP inhibitors [16-21]. Recently, as illustrated in Fig. 2, we have found the aromatic pyrazinyl urea derivatives to be inactive [18]. However, high activity has been exhibited by pyrazinyl thiourea analogs during our recent investigation for pyridyl/pyrazinyl thioureas [22]. Thus, we revisited the pyrazinyl urea chemical scaffold in order to identify a potential promising mPTP modulating analog. Herein, various aliphatic derivatives have been included in our investigation containing chloroethyl and piperazinethyl analogs as we noticed previously high activity of the pyridyl derivatives of these moieties. Successfully, in this report, the blocking activity of new seventeen pyrazinyl ureas against Aβ-induced mPTP opening has been found superior to that of the peptidic standard CsA. The most active hits were further assessed for their effect on ATP production as well as their protective effect against Aβ-induced ATP production impairment. The promising candidates were subjected to MTT viability to

evaluate their toxicity on neuronal cells. After assessment of cardiotoxicity, the promising compound **5** has been found to be a safe mPTP modulator that could serve as a novel runner towards AD drug development marathon.

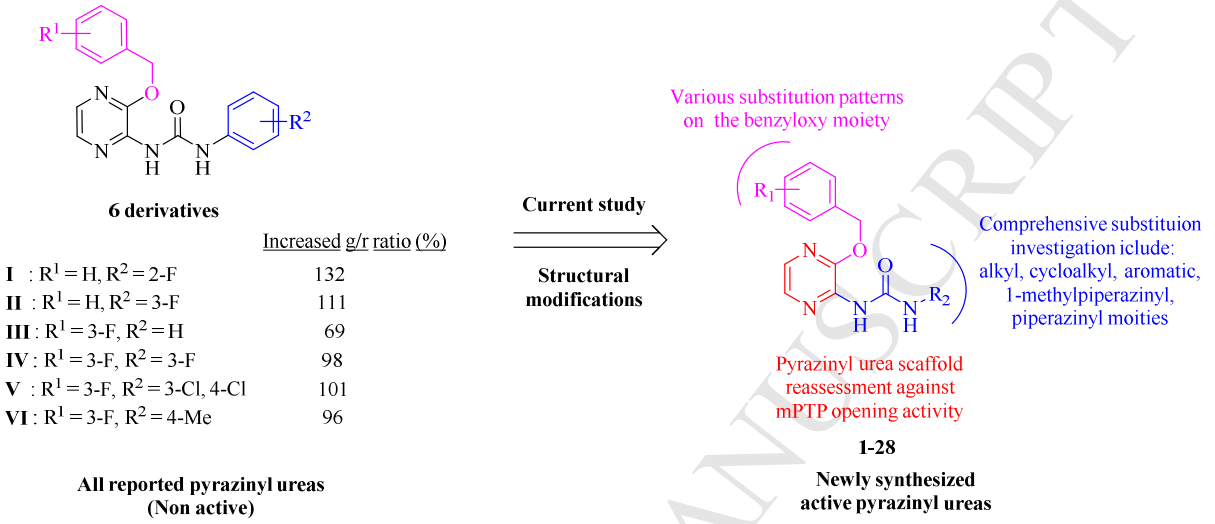

Fig. 2. KIST reported pyrazinyl ureas with low mPTP inhibition activity and revisiting design approach of the newly synthesized pyrazinyl ureas *via* modifying the eastern moiety as well as various substitutions on the benzyloxy group.

2. Results and discussion

2.1. Chemistry

A concise preparation of the target compounds (**1**−**28**) was achieved as illustrated in Scheme 1. Nucleophilic aromatic substitution of the commercially available starting material 2-amino-3-chloropyrazine (**VII**) with the appropriate phenylmethoxide derivative generated by treatment of the corresponding benzyl alcohol with sodium hydride afforded 3-aryloxypyrazin-2-amine derivatives (**VIIIa**−**f**). Nucleophilic addition of intermediates **VIII** to the appropriate electrophilic isocyanate derivative afforded the corresponding pyrazinyl ureas (**1**−**21**) while 2-chloroethyl urea analogs (**22**−**24**) were accessed *via* reaction of intermediates **VIIIa**, **VIIIc**, and **VIIId** with 2-chloroethyl isocyanate reagent in presence of DIPEA. Finally, a small series of

piperazinethyl urea derivatives (**25**−**28**) were obtained *via* reaction of 2-chloroethyl urea analogs (**22**−**24**) with the appropriate piperazine derivative.

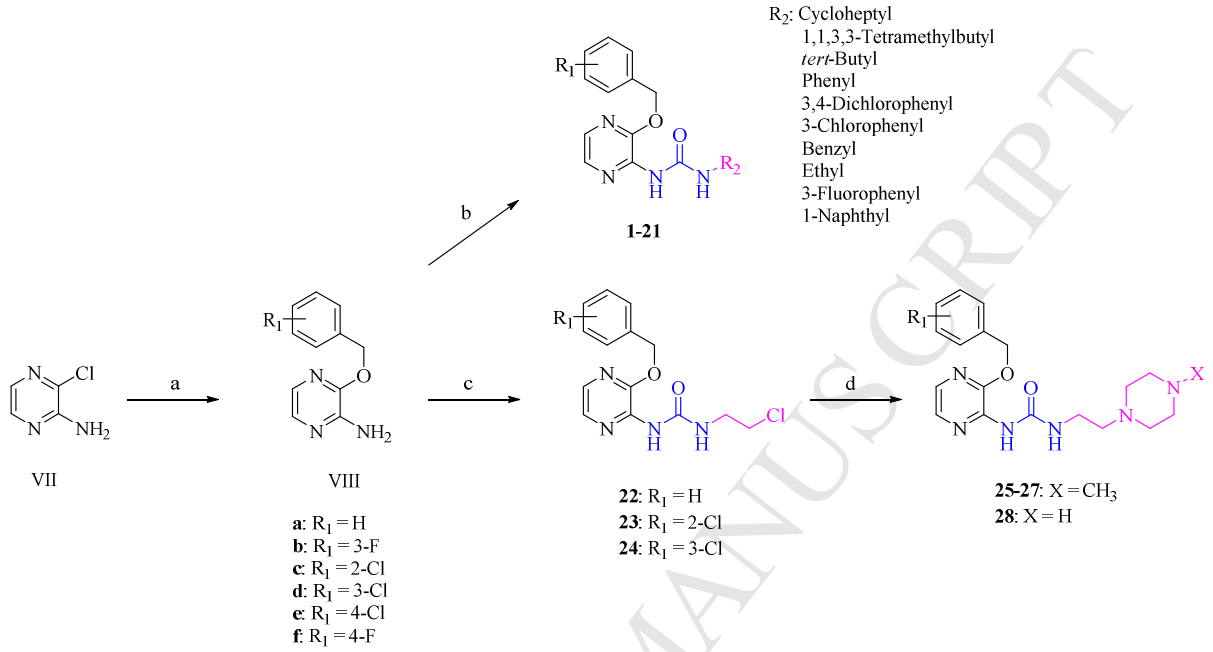

Scheme 1. Reagents and conditions: a) benzyl alcohol derivative, NaH (60% in mineral oil), DMF, 100 °C, 15 h; b) for aromatic urea derivatives: appropriate aromatic isocyanate derivative, THF, reflux, 3−6 h; for aliphatic urea derivatives: appropriate aliphatic isocyanate derivative, NaH (60% in mineral oil), THF, reflux 5h; c) 2-chloroethyl isocyanate, DIPEA, THF, reflux, 18 h; d) appropriate piperazine derivative, K_2CO_3, MeCN, reflux, 20 h.

2.2. Biological evaluation

2.2.1. Protection against loss of mitochondrial membrane potential assay (JC-1 assay)

As the mitochondrial membrane potential ($\Delta\Psi_M$) is essential to maintain the mitochondrial integrity, the prolonged opening of the mega-channel mPTP leads to mitochondrial membrane potential loss. While mitochondria with conserved membrane potential are featured with an inside negative matrix potential, the decline in mitochondrial membrane potential could be measured and quantified using fluorescent cationic dyes. JC-1 (5,5',6,6'-tetrachloro-1,1',3,3'-tetraethylbenzimidazolocarbocyanine iodide); a lipophilic cationic cyanine dye; offers many advantages over other cationic dyes as its performance is specific for the mitochondrial

membrane potential; it is not affected by other components including plasma membrane potential ($\Delta\Psi_p$), mitochondrial size or shape [23, 24]. In mitochondria with conserved membrane potential, JC-1 forms red aggregates which break up into green fluorescing monomers upon membrane potential loss. Using the neurotoxin amyloid beta (Aβ), the protective effect of the newly synthesized compounds to inhibit the Aβ-induced mitochondrial potential loss was successfully quantified *via* measurement of the green/red fluorescence ratio in hippocampal neuronal cells. In this assay, the standard Cyslosporin (CsA) lowered the green/red (g/r) ratio to 46% (recovery of the mitochondrial membrane potential = 54%). As illustrated in Table 1, both of aromatic and aliphatic derivatives possessing unsubstituted benzyloxy moiety (compounds **1**−**5**) elicited significant reduction of g/r ratio. However, the *t*-butyl derivative **3** was the less effective among them eliciting g/r % higher than the standard CsA. While, the phenyl derivative **4** was almost as active as the standard CsA. A slightly different pattern of activity was elicited by compounds having 3-flourobenzyloxy moiety (compounds **6**−**9**). Among the later derivatives, the *t*-butyl derivative **7** was also the less effective among them eliciting g/r % higher than the standard CsA. However, the phenyl derivative **8** showed increased activity. In contrast, the *t*-butyl derivative **11** was the most active while the 1,1,3,3-tetramethylbutyl derivative **10** became the less active among the derivatives having 2-chlorobenzyloxy moiety (compounds **10**−**14**). For the 3-chlorobenzyloxy derivatives (compounds **15**−**18**), ethylurea derivative **15** was the less active than aromatic congeners. Converting the ethyl substituent of compound **15** into 2-chloroethyl derivative **24** produced less active compound. However, attachment of *N*-methylpiperazinyl moiety instead of the chlorine atom of compound **24** resulted in the more active compound **27**. Similarly, replacement of chlorine atom of compound **23** with piperazinyl or *N*-methylpiperazinyl resulted in the more active compounds **28** and **26**. This pattern of activity

enhancement by replacing the chlorine atom with *N*-methylpiperazinyl moiety was less pronounced for compounds **22** and **25** having unsubstituted benzyloxy moiety. Among all evaluated compounds, derivative **21** possessing 4-fluorobenzyloxy moiety and 1,1,3,3-tetramethylbutylurea moiety was the most effective eliciting 17% g/r ratio. Also, another five compounds (**2**, **5**, **6**, **11**, and **18**) showed high efficiency with increased g/r ratio less than 30%. In addition, only four compounds (**15**, **20**, **23**, and **24**) exerted weak or non-significant inhibitory activity ranging from 60~73%. Overall investigation shows that pyrazine-based scaffold could results in potentially active chemical entities. However, the mixed activity might indicate that subtle stereoelectronic variations significantly impact the elicited biological activity [25, 26]. Accordingly, to characterize the promising hit compounds among the synthesized series, a set of active compounds were further assessed for ATP production (Luciferase-based assay) as well as neurocytotoxicity assay.

Table 1. *In vitro* blocking activity of the newly synthesized compounds (**1**−**28**) against Aβ-induced mPTP opening in hippocampal neuronal cell line HT-22 (JC-1 assay) at dose of 5 µM

Cpd	R_1	R_2	Increased g/r ratio (%)[a]	Cpd	R_1	R_2	Increased g/r ratio (%)[a]
1	H	Cycloheptyl	33	**16**	3-Cl	Phenyl	59
2	H	1,1,3,3-Tetramethylbutyl	25	**17**	3-Cl	3-Fluorophenyl	50
3	H	*tert*-Butyl	51	**18**	3-Cl	3-Chlorophenyl	29
4	H	Phenyl	44	**19**	4-Cl	1,1,3,3-Tetramethylbutyl	35
5	H	3,4-Dichlorophenyl	29	**20**	4-Cl	1-Naphthyl	60
6	3-F	1,1,3,3-Tetramethylbutyl	29	**21**	4-F	1,1,3,3-Tetramethylbutyl	17
7	3-F	*tert*-Butyl	55	**22**	H	−	53
8	3-F	Phenyl	30	**23**	2-Cl	−	72
9	3-F	3-Chlorophenyl	39	**24**	3-Cl	−	73
10	2-Cl	1,1,3,3-Tetramethylbutyl	59	**25**	H	−	43
11	2-Cl	*tert*-Butyl	28	**26**	2-Cl	−	34
12	2-Cl	Benzyl	33	**27**	3-Cl	−	34
13	2-Cl	Phenyl	39	**28**	2-Cl	−	37
14	2-Cl	3-Chlorophenyl	55	**CsA**	−	−	46
15	3-Cl	Ethyl	60				

[a] % Increase of fluorescence-ratio (green/red) after treatment of each compound and Aβ with regard to that of Aβ alone (100%). See the text for more detailed information. All data are reported as the average of duplicates.

2.2.2. Assessment of ATP production and protection against Aβ-induced impairment of ATP production (Luciferase-based assay)

Mitochondrial toxicity is a major concern for safety in drug discovery programs; in addition, the compounds developed in this work are potential mPTP blockers whose core unit is formed of ATP synthase dimers. Therefore, it is important to assess their impact on mitochondrial ATP production to avoid undesirable blocking of mitochondrial energy production. Thus, a set of highly active compounds was evaluated for potential toxicity on ATP production using hippocampal neuronal cell line after incubation for 7 h with 5 µM concentrations of each tested compound. As shown in Table 2, compounds **11**, **13** and **28** were found to seriously impair the mitochondrial ATP production and, therefore, were excluded from further evaluation. Fortunately, in presence of other compounds of the evaluated set, mitochondria elicited ATP production levels close or higher than the level of ATP production in presence of the standard piracetam. In lieu of this, it may be concluded that these compounds does not produce unwanted impairment of mitochondrial energy production. Next, the compounds passed mitochondrial ATP production filter were assessed for their capacity to protect neuronal cells against Aβ-induced deterioration of ATP production which is a major concern in of Aβ-induced mitochondrial dysfunction. As illustrated in Fig. 3 and presented in Table 2, three compounds (**1**, **5**, and **12**) were able to show significant promising protection against Aβ-suppression of ATP production with 45.7, 71.2, and 71.3% of ATP recovery respectively.

Table 2. The result of ATP assay of the tested compounds

Cpd	ATP Production[a]	% ATP Recovery[b]	Cpd	ATP Production[a]	% ATP Recovery[b]
1	103.4	45.7	**18**	85.4	-3.5

2	86.0	-59.0	**19**	85.7	-1.7
5	148.6	71.2	**25**	97.2	0.7
6	98.9	32.9	**27**	96.1	17.7
11	55.3	NT[c]	**28**	70.0	NT[c]
12	96.9	71.3	Piracetam	88	127
13	66.9	NT[c]			

[a] % ATP production in hippocampal neuronal cell line HT-22 after 7 h incubation with 5 µM of each compound. All data are reported as the average of duplicates.
[b] % Recovery of ATP production by Aβ-suppressed mitochondrial ATP production in hippocampal neuronal cell line HT-22 after 7 h incubation with 5 µM of each compound. All data are reported as the average of duplicates.
[c] NT: not tested

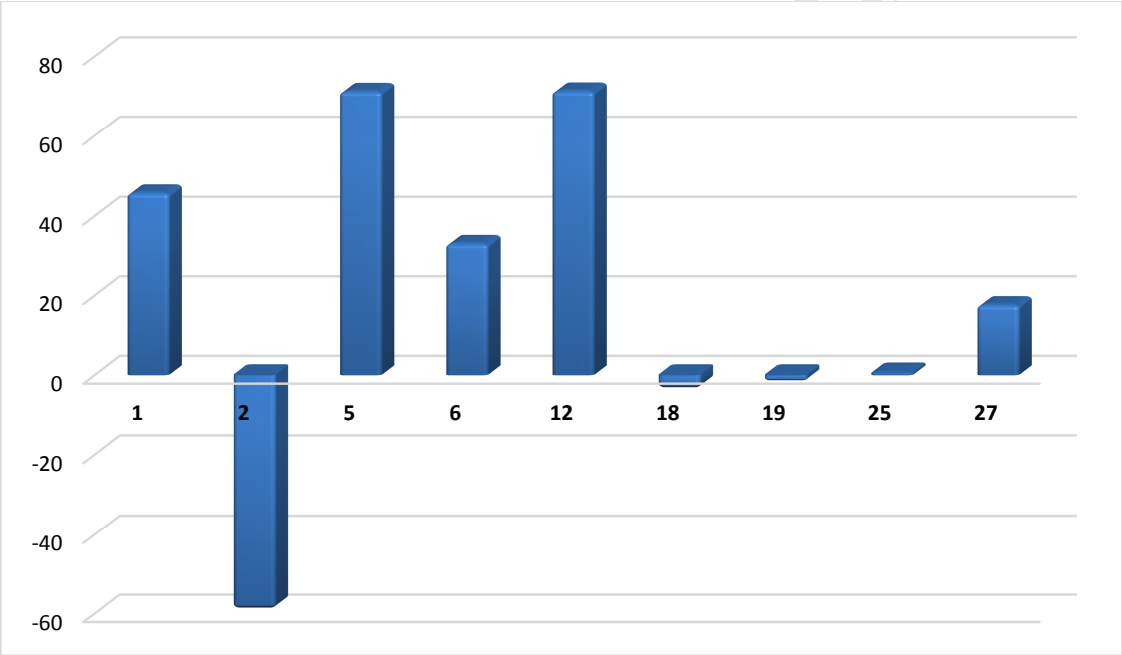

Fig. 3. The result of % recovery of ATP production assay at 5 µM of each compound against Aβ-suppressed mitochondrial ATP reduction

2.2.3. Assessment of neurocytotoxicity (MTT assay)

As a subsequent filter to exclude compound(s) possessing potential cytotoxic effects [27, 28], analogs showed promising results in luciferase-based assay (**1**, **5**, and **12**) were subjected to MTT cell viability assay to evaluate the level of hippocampal neuronal cells survival after incubation for 24 h with 5 µM of each tested compound. As presented in Table 3, compound **1** elicited potential cytotoxic effects decreasing the cells viability to 59%. Also, compound **12** elicited a

slight decrement in cell viability, to a lesser extent that is comparable to that of the standard CsA. Fortunately, compound **5** showed cell viability result superior to that of CsA and piracetam. Based on previous applied consecutive filter assays, it can be assumed that this derivative has no direct toxic effect on mitochondrial ATP production and also no cytotoxicity on hippocampal neuronal cells viability. In addition, it has a significant protection feature against Aβ-induced impairment of ATP production.

Table 3. Results of neurocytotoxicity at 5 µM concentrations

Cpd	MTT viability[a]
1	59
5	139.2
12	84.8
Piracetam	132
CsA	90

[a] % Viability of hippocampal neuronal cell line HT-22 after 24 h incubation with 5 µM of each compound. All data are reported as the average of duplicates.

2.2.4. Assessment of cardiotoxicity (hERG channel assay)

Blockade of the human ether-a-go-go related gene (hERG) potassium channel may cause sudden drug withdrawal from markets as a result of induction the prolongation of the QT interval of the surface electrocardiogram (ECG) which makes hERG blockade an important hurdle in lead optimization activity as well as drug discovery process due to its potential cardiotoxicity [29, 30]. Thus, we measured the hERG inhibitory activity of compound **5**. The test demonstrated a high micromolar IC_{50} value equal to 11.3 µM. Hence, compound **5** doesn't exert potential blockage activity towards the hERG channel. Accordingly, it could be assumed as safe compound with regard to the potential cardiotoxicity.

2.2.5. Molecular modelling

In the reported crystal of human CypD-CsA complex (pdb ID = 2Z6W), CsA effectively binds to CypD eliciting hydrophobic interactions as a major contributor to the binding forces [31]. The hydrophobic pocket 1 formed by residues Met61, Ala101, Phe113, Leu122 and His126 interacts with the methylated valine (Mva11) of CsA. Amino acid residues Gln63 and Asn102 form a saddle between pocket 1 and the less hydrophobic pocket 2. Also, the structure of CypD-CsA complex shows that Phe60, Ile57 and Trp121 form a flat hydrophobic surface which interacts with the side chain methylated leucine (Mle9) of CsA. In the crystal structure, hydrogen bonds exist with amino acids Gln63 and Asn102 in the saddle region, Arg55 and His126 at the edge of pocket 1, and Trp121 in the flat hydrophobic surface.

To get insights into the molecular behavior underlying the differences in the elicited biological activities, a molecular modeling study was conducted. A set of active compounds (**2**, **5**, **6**, **11**, **18** and **21**), as well as, another set of the less active compounds (**15**, **20**, **23** and **24**) were docked into the reported crystal structure of human CypD (pdb ID = 2Z6W). The retrieved poses were refined using *in situ* minimization after which, the energetic terms of CypD-ligand complex were calculated. Poses were ranked based on these calculated energetic terms. As reported earlier, the obtained poses of this class of compounds could accommodate two general binding modes [18, 19, 22]. The first binding mode, favored by active compounds, features the ligand partially buried into the hydrophobic pocket 1 eliciting favorable hydrophobic interactions. The second binding mode, favored by inactive compounds, shows a vacant hydrophobic pocket 1 while the ligand is forming an umbrella above it.

Analysis of compound **5** poses which represent the set of the most active compounds shows a strong tendency of this compound to bind in mode 1. According to the performed *in silico* calculations, the pyrazine ring in binding mode 1 shown in Fig. 4A fits into the hydrophobic pocket 1 eliciting favorable hydrophobic interactions with the aromatic rings of Phe113 and His126, as well as, with the side chain of Ala101. Also, the pyrazine ring is involved in electrostatic π-cation interaction with His126. In addition, it establishes hydrogen bonding interactions with side chain of Arg55 and backbone peptide linkage of Asn102. Meanwhile, the urea moiety accepts hydrogen bond from His126 and donates two hydrogen bonds to Asn102. In addition, there is an amide-π stacking interaction between the aromatic ring of the 3,4-dichlorophenyl moiety and the peptide linkage of Ala103-Gly104. Moreover, the two chlorine atoms are involved in two hydrophobic interactions with side chains of Pro105 and Lys125. The calculated energetic terms for this binding mode were -58.68 Kcal/mol for binding energy and 1.80 Kcal/mol for the value of the ligand conformational energy above the energy of the lowest conformer energy. On the other hand, as illustrated in Fig. 4B, if compound **5** accommodates binding mode 2 in which it is hovering above the hydrophobic pocket 1 without docking inside, it would interact through several favorable interactions including interactions of the 3,4-dichlorophenyl moiety with hydrophobic and π-cation interactions with His126, as well as, hydrophobic interactions of the two chlorine atoms with Phe60 and Leu122. The urea moiety donates two hydrogen bonds to Asn102 while the pyrazine ring is interacting via two hydrogen bonds with Gln63and Gln111, in addition to π-cation and hydrophobic interactions with arg55 and Ala101 respectively. *In silico* calculations of the energetic terms of binding mode 2 for compound **5** estimated binding energy value of -54.75 Kcal/mol and ligand conformational energy above the energy of the lowest conformer energy of 2.74 Kcal/mol. The higher

conformational energy of the conformer required for binding mode 2 relative to that required for binding mode 1 translates into less accessibility of the conformer of binding mode 2. At the same time, the lower binding energy of binding mode 2 relative to that of binding mode 1 translates into lower kinetics for forming binding mode 2. Considering the above mentioned energetic terms, the high efficiency of compound **5** in reducing g/r ratio would be understandable.

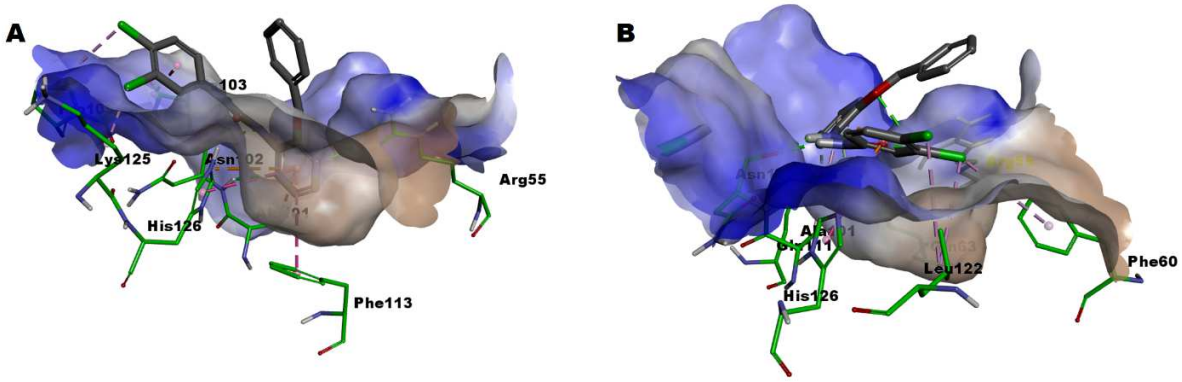

Fig. 4. Binding modes of compound **5** with CypD: A) Binding mode 1; B) Binding mode 2

Analysis of compound **23** poses representing the set of the less active compounds shows that if it binds according to binding mode 1 (Fig. 5A), it would elicit favorable hydrogen bonding interactions between pyrazine ring and all of Arg55, Gln63 and His126. It shows also hydrophobic and π-sulfur interactions with Ala101 and Met61, respectively. The urea moiety accepts hydrogen bonds from Arg55 while the oxygen atom of the benzyloxy moiety accepts hydrogen bonding from His126. In comparison, the predicted binding mode 2 of compound **23** (Fig. 5B) shows favorable hydrogen bonding between Arg55 and both of the pyrazine ring and oxygen atom of the urea moiety, as well as, hydrophobic and π-cation interactions between His126 and the aromatic ring of the benzyloxy moiety. In addition, the chloro atom of the benzyloxy moiety interacts hydrophobically with Lys125. The energetic terms for binding mode 1 of compound **23** were estimated to be -57.60 Kcal/mol for binding energy, -3050.51 Kcal/mol

for ligand-complex energy and 3.75 Kcal/mol for conformational energy above the energy of the lowest conformer energy. Regarding binding mode 2 of compound **23**, the energetic terms of binding mode 2 were estimated to be -46.31 for Kcal/mol binding energy, -3057.89 Kcal/mol for ligand-complex energy and 1.82 Kcal/mol for ligand conformational energy above the energy of the lowest conformer energy. While the lower binding energy of mode 2 relative to mode 1 predicts slower kinetics for formation of binding mode 2, the lower conformational energy of the conformer of binding mode 2 indicates more probability of accessing that conformer. In addition, the lower ligand-CypD complex energy predicts more stability of binding mode 2 and thus more elapsed time accommodating this binding mode. In the light of these calculations, the lower efficiency of compound **23** would be justifiable.

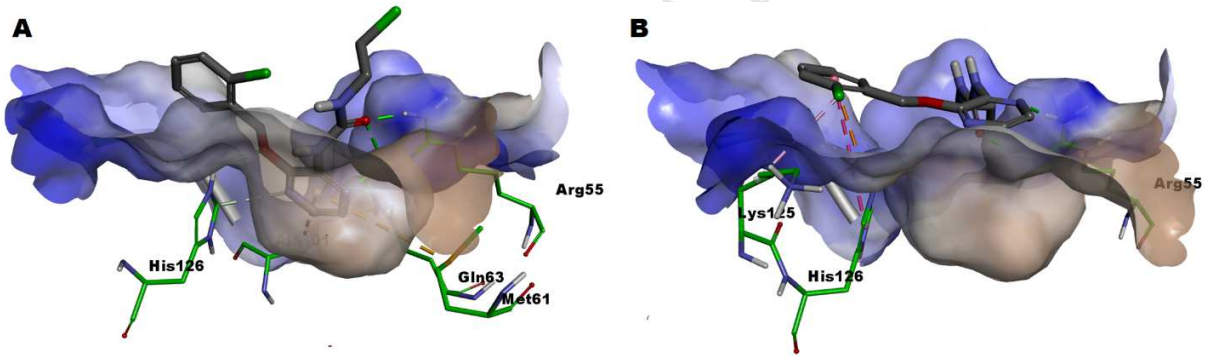

Fig. 5. Binding modes of compound **23** with CypD: A) Binding mode 1; B) Binding mode 2

3. Conclusion

As a conclusion for revisiting of the pyrazinyl-urea chemistry as potential modulators of Aβ-induced mitochondrial dysfunction towards novel therapies for Alzheimer's diseases, compound **5**, 1-(3-(benzyloxy)pyrazin-2-yl)-3-(3,4-dichlorophenyl)urea, has been identified as a new promising candidate featured with: (1) significant blockage of mPTP Aβ-induced opening (2) no toxicity on ATP production (3) no detrimental effect on the viability of hippocampal neuronal cells (4) significant protection against Aβ-induced impairment of ATP production (5) no

potential cardiotoxicity. Thus, this study presents analog **5** as a new non-peptidyl pyrazinyl-urea-based promising mPTP blocker.

4. Experimental

4.1. Chemistry

General: All reactions and manipulations were performed in nitrogen atmosphere using standard Schlenk techniques. The reaction solvents and reagents were purchased from commercial suppliers and used without further purification. The NMR spectra were obtained on Bruker Avance 300 or 400. ^{1}H NMR spectra were referenced to tetramethylsilane (δ = 0.00 ppm) as an internal standard and are reported as follows: chemical shift, multiplicity (br = broad, s = singlet, d = doublet, t = triplet, dd = doublet of doublet, m = multiplet). Column chromatography was performed on Merck Silica Gel 60 (230−400 mesh) and eluting solvents for all of these chromatographic methods are noted as appropriated-mixed solvent with given volume-to-volume ratios. TLC was carried out using glass sheets pre-coated with silica gel 60 F_{254} purchased by Merk. The purity of samples was determined by analytical HPLC using a Water ACQUITY UPLC (CORTECS^{TM}) with C18 column (2.1 mm x 100 mm; 1.6 µm) at temperature 40 °C. HPLC data were recorded using parameters as follows: 0.1% formic acid in water and 0.1% formic acid in methanol and flow rate of 0.3 mL/min. For more details, see supplementary file. High-resolution spectra were performed on Waters ACQUITY UPLC BEH C18 1.7µ−Q-TOF SYNAPT G2-Si High Definition Mass Spectrometry.

4.1.1. General procedure of 3-(benzyloxy)pyrazin-2-amine derivatives (VIIIa−f)

NaH (60% in mineral oil, 0.04 g, 1 mmol) was added to a stirred solution of the appropriate benzyl alcohol derivative (1 mmol) in anhydrous DMF (3 mL) at room temperature and stirring was continued for 1 h. Commercially available 2-amino-3-chloropyrazine (0.13 g, 1 mmol) was added to the reaction mixture which was further stirred at 100 °C for 15 h. After cooling, the solvent was evaporated and the residue was partitioned between water and dichloromethane. The organic layer was dried over anhydrous Na_2SO_4, filtered, and concentrated. The residue was purified by flash column chromatography (SiO_2, EA/*n*-Hex = 1/5). Synthesis and characterization of compounds **VIIIa−c** have been reported previously by our group [18, 19].

3-(3-Chlorobenzyloxy)pyrazin-2-amine (VIIId)

Light yellow solid, yield: 66.0%, ^{1}H NMR (400 MHz, $CDCl_3$) δ = 4.80 (2H, brs, NH_2), 5.37 (2H, s, OCH_2Ph), 7.31 (3H, d, *J* = 1.3 Hz, ArH), 7.42 (1H, d, *J* = 3.1 Hz, ArH), 7.44 (1H, s, ArH), 7.58 (1H, d, *J* = 3.1 Hz, ArH).

3-(4-Chlorobenzyloxy)pyrazin-2-amine (VIIIe)

White solid, yield: 38.1%, ^{1}H NMR (400 MHz, $CDCl_3$) δ = 5.36 (2H, s, OCH_2Ph), 6.31 (2H, brs, NH_2), 7.25 (1H, d, *J* = 3.0 Hz, ArH), 7.44 (2H, d, *J* = 8.4 Hz, ArH), 7.48 (1H, d, *J* = 3.0 Hz, ArH), 7.52 (2H, d, *J* = 8.4 Hz, ArH).

3-(4-Fluorobenzyloxy)pyrazin-2-amine (VIIIf)

Yellow solid, yield: 65.5%, ^{1}H NMR (400 MHz, $CDCl_3$) δ = 4.78 (2H, brs, NH_2), 5.36 (2H, s, OCH_2Ph), 7.05−7.09 (2H, m, ArH), 7.41−7.44 (3H, m, ArH), 7.56 (1H, d, *J* = 3.1 Hz, ArH).

4.1.2. General procedure of pyrazinyl urea compounds 1−21

For aromatic urea derivatives; the appropriate aromatic isocyanate (3.0 mmol) was added to a solution of the appropriate 2-amino-3-benzyloxy pyrazine derivative (2.5 mmol) in THF (10 mL). The reaction was refluxed for 3−6 h. After cooling, the reaction mixture was evaporated and the residue was purified by precipitation in cold methanol and filtered to give the target compound(s). For aliphatic urea derivatives; the appropriate aliphatic isocyanate derivative (1.02 mmol) was added to a solution of the appropriate 2-amino-3-benzyloxy pyrazine derivative (0.85 mmol) in dry THF (5 mL) in the presence of NaH (60% in mineral oil, 68 mg, 1.71 mmol). The reaction was refluxed for 5 h. After cooling, the reaction mixture was evaporated and the residue was purified by flash column chromatography (SiO_2, EA/*n*-Hex = 1/4).

1-(3-(Benzyloxy)pyrazin-2-yl)-3-cycloheptylurea (1)

White solid, yield: 46.2%, mp: 91.8-93.7 °C, HPLC purity: 7.33 min, 100%, ^{1}H NMR (400 MHz, $CDCl_3$) δ = 1.58−1.65 (10H, m, $5CH_2$), 1.96−2.00 (2H, m, CH_2), 3.97−4.03 (1H, m, CH), 5.41 (2H, s, OCH_2Ph), 7.29 (1H, s, NH), 7.36−7.44 (5H, m, ArH), 7.63 (1H, d, *J* = 3.1 Hz, ArH), 7.66 (1H, d, *J* = 3.1 Hz, ArH), 9.08 (1H, s, NH). ^{13}C NMR (100 MHz, $CDCl_3$) δ = 24.00, 27.96, 35.12, 50.96, 68.72, 128.61, 128.67, 131.51, 131.64, 135.48, 140.10, 147.90, 153.22. HRMS (ES^+): *m/z* calculated for $C_{19}H_{24}N_4O_2$: 341.1977 $[M+H]^+$. Found 341.1976.

1-(3-(Benzyloxy)pyrazin-2-yl)-3-(2,4,4-trimethylpentan-2-yl)urea (2)

White solid, yield: 20.1%, mp: 86.7-87.1 °C, ^{1}H NMR (400 MHz, $CDCl_3$) δ = 1.01 (9H, s, $3CH_3$), 1.47 (6H, s, $2CH_3$), 1.80 (2H, s, CH_2), 5.40 (2H, s, OCH_2Ph), 7.15 (1H, s, NH),

7.35−7.43 (5H, m, ArH), 7.61 (1H, d, *J* = 3.1 Hz, ArH), 7.63 (1H, d, *J* = 3.1 Hz, ArH), 9.05 (1H, s, NH). HRMS (ES^+): *m/z* calculated for $C_{20}H_{28}N_4O_2$: 357.2290 $[M+H]^+$. Found 357.2291.

1-(3-(Benzyloxy)pyrazin-2-yl)-3-(*tert*-butyl)urea (3)

Yellow solid, yield: 16.3%, mp: 96.9-97.7 °C, HPLC purity: 6.77 min, 100%, ^1H NMR (400 MHz, $CDCl_3$) δ = 1.43 (9H, s, $3CH_3$), 5.41 (2H, s, OCH_2Ph), 7.18 (1H, s, NH), 7.36−7.43 (5H, m, ArH), 7.61 (1H, d, *J* = 3.1 Hz, ArH), 7.65 (1H, d, *J* = 3.1 Hz, ArH), 9.01 (1H, s, NH). ^{13}C NMR (100 MHz, $CDCl_3$) δ = 29.06, 50.74, 68.65, 128.48, 128.52, 128.65, 131.31, 131.57, 135.55, 140.21, 147.84, 152.77. HRMS (ES^+): *m/z* calculated for $C_{16}H_{20}N_4O_2$: 301.1664 $[M+H]^+$. Found 301.1667.

1-(3-(Benzyloxy)pyrazin-2-yl)-3-phenylurea (4)

White solid, yield: 91.8%, mp: 139.4-140.0 °C, HPLC purity: 6.80 min, 100%, ^1H NMR (400 MHz, $CDCl_3$) δ = 5.43 (2H, s, OCH_2Ph), 7.09 (1H, t, *J* = 7.4 Hz, ArH), 7.33 (2H, t, *J* = 7.5 Hz, ArH), 7.36−7.45 (5H, m, ArH), 7.49 (1H, s, NH), 7.57 (2H, dd, *J* = 1.1 Hz, 8.6 Hz, ArH), 7.72 (2H, dd, *J* = 3.1 Hz, 14.8 Hz, ArH), 11.28 (1H, s, NH). ^{13}C NMR (100 MHz, $CDCl_3$) δ = 68.99, 120.37, 123.88, 128.70, 128.75, 129.01, 131.45, 132.35, 135.34, 138.01, 139.50, 148.08, 151.63. HRMS (ES^+): *m/z* calculated for $C_{18}H_{16}N_4O_2$: 321.1351 $[M+H]^+$. Found 321.1349.

1-(3-(Benzyloxy)pyrazin-2-yl)-3-(3,4-dichlorophenyl)urea (5)

White solid, yield: 87.1%, mp: 151.1-151.8 °C, HPLC purity: 7.65 min, 100%, ^1H NMR (400 MHz, $CDCl_3$) δ = 5.44 (2H, s, OCH_2Ph), 7.32−7.45 (7H, m, ArH), 7.53 (1H, s, NH), 7.73-7.74 (2H, m, ArH), 7.76 (1H, d, *J* = 2.4 Hz, ArH), 11.42 (1H, s, NH). ^{13}C NMR (100 MHz, $CDCl_3$) δ

= 69.08, 119.37, 121.63, 126.80, 128.70, 128.75, 130.41, 131.30, 132.65, 132.80, 135.23, 137.64, 139.09, 148.10, 151.36. HRMS (ES^+): *m/z* calculated for $C_{18}H_{14}Cl_2N_4O_2$: 389.0572 $[M+H]^+$. Found 389.0570.

1-(3-(3-Fluorobenzyloxy)pyrazin-2-yl)-3-(2,4,4-trimethylpentan-2-yl)urea (6)

White solid, yield: 56.2%, mp: 112.5-113.8 °C, HPLC purity: 7.83 min, 100%, ^{1}H NMR (400 MHz, $CDCl_3$) δ = 1.02 (9H, s, $3CH_3$), 1.48 (6H, s, $2CH_3$), 1.81 (2H, s, CH_2), 5.40 (2H, s, OCH_2Ph), 7.04 (1H, td, *J* = 2.2 Hz, 8.4 Hz, ArH), 7.11−7.14 (2H, m, ArH+NH), 7.20 (1H, d, *J* = 7.7 Hz, ArH), 7.32−7.38 (1H, m, ArH), 7.60 (1H, d, *J* = 3.1 Hz, ArH), 7.65 (1H, d, *J* = 3.1 Hz, ArH), 9.04 (1H, s, NH); ^{13}C NMR (100 MHz, $CDCl_3$) δ = 29.57, 31.47, 31.65, 51.68, 54.52, 67.75, 115.31 (J_{C-F} = 21.7 Hz), 115.44 (J_{C-F} = 20.8 Hz), 123.88, 130.26 (J_{C-F} = 8.0 Hz), 131.25, 131.78, 138.00 (J_{C-F} = 7.3 Hz), 140.11, 147.48, 152.51, 162.83 (J_{C-F} = 245.2 Hz). HRMS (ES^+): *m/z* calculated for $C_{20}H_{27}FN_4O_2$: 375.2196 $[M+H]^+$. Found 375.2198.

1-(3-(3-Fluorobenzyloxy)pyrazin-2-yl)-3-(*tert*-butyl)urea (7)

White solid, yield: 75.9%, mp: 102.8-103.5 °C, HPLC purity: 6.78 min, 100%, ^{1}H NMR (400 MHz, $CDCl_3$) δ = 1.43 (9H, s, $3CH_3$), 5.40 (2H, s, OCH_2Ph), 7.03−7.05 (1H, m, ArH), 7.10−7.13 (1H, m, ArH), 7.15 (1H, s, NH), 7.19 (1H, *J* = 7.4 Hz, ArH), 7.32−7.36 (1H, m, ArH), 7.60 (1H, d, *J* = 3.1 Hz, ArH), 7.66 (1H, d, *J* = 3.1 Hz, ArH), 8.99 (1H, s, NH); ^{13}C NMR (100 MHz, $CDCl_3$) δ = 29.60, 50.77, 67.71, 115.42 (J_{C-F} = 21.5 Hz), 115.42 (J_{C-F} = 20.9 Hz), 123.87, 130.25 (J_{C-F} = 8.0 Hz), 131.27, 131.85, 137.99, 140.13, 147.51, 152.71, 162.83 (J_{C-F} = 245.6 Hz). HRMS (ES^+): *m/z* calculated for $C_{16}H_{19}FN_4O_2$: 319.1510 $[M+H]^+$. Found 319.1577.

1-(3-(3-Fluorobenzyloxy)pyrazin-2-yl)-3-phenylurea (8)

White solid, yield: 51.9%, mp: 136.0-136.5 °C, HPLC purity: 6.80 min, 100%, ^{1}H NMR (400 MHz, $CDCl_3$) δ = 5.43 (2H, s, OCH_2Ph), 7.03−7.16 (3H, m, ArH), 7.22 (1H, d, *J* = 7.7 Hz, ArH), 7.31−7.37 (3H, m, ArH), 7.50 (1H, s, NH), 7.58 (2H, dd, *J* = 1.1 Hz, 8.7 Hz, ArH), 7.70 (1H, d, *J* = 3.1 Hz, ArH), 7.76 (1H, d, *J* = 3.1 Hz, ArH), 11.26 (1H, s, NH). ^{13}C NMR (100 MHz, $CDCl_3$) δ = 68.04, 115.44 (J_{C-F} = 13.1 Hz), 115.65 (J_{C-F} = 12.1 Hz), 120.38, 123.93, 124.08 (J_{C-F} = 3.0 Hz), 129.00, 130.36 (J_{C-F} = 9.1 Hz), 131.73, 132.30, 137.81 (J_{C-F} = 7.0 Hz), 137.95, 139.46, 147.78, 151.58, 162.87 (J_{C-F} = 246.5). HRMS (ES^+): *m/z* calculated for $C_{18}H_{15}FN_4O_2$: 339.1257 $[M+H]^+$. Found 339.1271.

1-(3-(3-Fluorobenzyloxy)pyrazin-2-yl)-3-(3-chlorophenyl)urea (9)

White solid, yield: 91.9%, mp: 146.5-147.4 °C, ^{1}H NMR (400 MHz, DMSO-d_6) δ = 5.49 (2H, s, OCH_2Ph), 6.86−6.90 (1H, m ArH), 7.17 (1H, td, *J* = 1.9 Hz, 8.4 Hz, ArH), 7.29−7.49 (5H, m, ArH), 7.61 (1H, dt, *J* = 2.1 Hz, 11.68 Hz, ArH), 7.83 (1H, d, *J* = 3.0 Hz, ArH), 7.95 (1H, d, *J* = 3.0 Hz, ArH), 9.16 (1H, s, NH), 11.09 (1H, s, NH). ^{13}C NMR (100 MHz, $CDCl_3$) δ = 68.13, 115.53 (J_{C-F} = 21.6 Hz), 115.68 (J_{C-F} = 21.1 Hz), 118.26, 120.25, 123.89, 124.11, 129.98, 130.38 (J_{C-F} = 9.4 Hz), 131.66, 132.59, 134.61, 139.25, 147.82, 151.38, 162.85 (J_{C-F} = 245.4 Hz).

1-(3-(2-Chlorobenzyloxy)pyrazin-2-yl)-3-(2,4,4-trimethylpentan-2-yl)urea (10)

White solid, yield: 86.1%, mp: 100.0-101.2 °C, ^{1}H NMR (400 MHz, $CDCl_3$) δ = 1.02 (9H, s, $3CH_3$), 1.48 (6H, s, $2CH_3$), 1.80 (2H, s, CH_2), 5.51 (2H, s, OCH_2Ph), 7.14 (1H, s, NH), 7.28−7.31 (2H, m, ArH), 7.41-7.46 (2H, m, ArH), 7.61 (1H, d, *J* = 3.1 Hz, ArH), 7.66 (1H, d, *J* = 3.1 Hz, ArH), 9.05 (1H, s, NH). ^{13}C NMR (100 MHz, $CDCl_3$) δ = 29.58, 31.48, 31.64, 51.68,

54.51, 66.03, 126.98, 129.73, 129.85, 130.17, 131.34, 131.73, 133.26, 133.97, 140.10, 147.56, 152.56.

1-(3-(2-Chlorobenzyloxy)pyrazin-2-yl)-3-(*tert*-butyl)urea (11)

White solid, yield: 85.2%, mp: 149.8-153.3 °C, ^{1}H NMR (400 MHz, $CDCl_3$) δ = 1.43 (9H, s, $3CH_3$), 5.51 (2H, s, OCH_2Ph), 7.16 (1H, brs, NH), 7.28−7.33 (2H, m, ArH), 7.41−7.45 (2H, m, ArH), 7.61 (1H, d, *J* = 3.1 Hz, ArH), 7.66 (1H, d, *J* = 3.1 Hz, ArH), 9.01 (1H, s, NH); ^{13}C NMR (100 MHz, $CDCl_3$) δ = 29.06, 50.77, 66.05, 126.98, 129.76, 129.88, 130.18, 131.36, 131.80, 133.26, 134.01, 140.12, 147.60, 152.76.

1-Benzyl-3-(3-(2-chlorobenzyloxy)pyrazin-2-yl)urea (12)

White solid, yield: 80.0%, mp: 107.8-108.8 °C, ^{1}H NMR (400 MHz, $CDCl_3$) δ = 4.53 (2H, d, *J* = 5.8 Hz, CH_2Ph), 5.44 (2H, s, OCH_2Ph), 7.19−7.28 (7H, m, ArH+NH), 7.34−7.39 (3H, m, ArH), 7.57 (2H, s, ArH), 9.38 (1H, s, NH). ^{13}C NMR (100 MHz, $CDCl_3$) δ = 43.88, 66.25, 127.03 127.26, 127.38, 128.63, 129.82, 130.02, 130.42, 131.87, 131.96, 133.16, 134.16, 138.81, 139.75, 147.74, 154.40.

1-(3-(2-Chlorobenzyloxy)pyrazin-2-yl)-3-phenylurea (13)

White solid, yield: 43.0%, mp: 198.8-196.7 °C, ^{1}H NMR (400 MHz, DMSO-d_6) δ = 5.54 (2H, s, OCH_2Ph), 7.06 (1H, t, *J* = 7.4 Hz, ArH), 7.33 (2H, dd, *J* = 7.6 Hz, 8.3 Hz, ArH), 7.38−7.40 (2H, m, ArH), 7.50−7.53 (1H, m, ArH), 7.56 (2H, d, *J* = 7.6 Hz, ArH), 7.71−7.73 (1H, m, ArH), 7.83 (1H, d, *J* = 3.0 Hz, ArH), 7.96 (1H, d, *J* = 3.0 Hz, ArH), 8.94 (1H, s, NH), 10.91 (1H, s, NH); ^{13}C

NMR (100 MHz, $CDCl_3$) δ = 66.43, 120.40, 123.92, 127.06, 129.01, 129.87, 130.11, 130.52, 131.67, 132.67, 133.05, 134.25, 137.96, 139.47, 147.88, 151.60.

1-(3-(2-Chlorobenzyloxy)pyrazin-2-yl)-3-(3-chlorophenyl)urea (14)

White solid, yield: 83.0%, mp: 169.5-170.6 °C, ^{1}H NMR (400 MHz, DMSO-d_6) δ = 5.54 (2H, s, OCH_2Ph), 7.11 (1H, d, *J* = 7.3 Hz, ArH), 7.33−7.40 (3H, m, ArH), 7.45 (1H, d, *J* = 8.7 Hz, ArH), 4.50−7.53 (1H, m, ArH), 7.71-7.73 (1H, m, ArH), 7.79 (1H, t, *J* = 2.0 Hz, ArH), 7.85 (1H, d, *J* = 2.9 Hz, ArH), 7.97 (1H, d, *J* = 2.9 Hz, ArH), 9.09 (1H, s, NH), 11.0 (1H, s, NH); ^{13}C NMR (100 MHz, $CDCl_3$) δ = 66.51, 118.25, 120.23, 123.86, 127.06, 129.89, 129.96, 130.16, 130.57, 131.59, 132.65, 132.98, 134.59, 139.25, 147.91, 151.41.

1-(3-(3-Chlorobenzyloxy)pyrazin-2-yl)-3-ethylurea (15)

White solid, yield: 65.2%, mp: 126.5-127.5 °C, ^{1}H NMR (300 MHz, DMSO-d_6) δ = 1.11 (3H, t, *J* = 7.2 Hz, CH_3), 2.26−7.27 (2H, m, CH_2), 5.42 (2H, s, OCH_2Ph), 7.37−7.44 (2H, m, ArH), 7.46−7.48 (1H, m, ArH), 7.67 (1H, brs, ArH), 7.71 (1H, d, *J* = 3.0 Hz, ArH), 7.80 (1H, d, *J* = 3.0 Hz, ArH), 8.52 (1H, s, NH), 8.81 (1H, s, NH); ^{13}C NMR (100 MHz, $CDCl_3$) δ = 15.25, 34.88, 67.79, 126.59, 128.62, 128.75, 129.99, 131.65, 131.91, 134.55, 137.48, 139.89, 147.57, 154.12.

1-(3-(3-Chlorobenzyloxy)pyrazin-2-yl)-3-phenylurea (16)

White solid, yield: 82.5%, mp: 148.0-148.5 °C, ^{1}H NMR (400 MHz, DMSO-d_6) δ = 5.46 (2H, s, OCH_2Ph), 7.06 (1H, t, *J* = 7.4 Hz, ArH), 7.33 (2H, t, *J* = 7.8 Hz, ArH), 7.40−7.44 (2H, m, ArH), 7.51 (1H, d, *J* = 6.6 Hz, ArH), 7.57 (2H, d, *J* = 8.2 Hz, ArH), 7.69 (1H, s, ArH), 7.81 (1H, d, *J* = 3.0 Hz, ArH), 7.93 (1H, d, *J* = 3.0 Hz, ArH), 9.05 (1H, s, NH), 10.97 (1H, s, NH); ^{13}C NMR

(100 MHz, $CDCl_3$) δ = 68.01, 120.40, 123.94, 126.67, 128.71, 128.86, 129.01, 130.06, 131.75, 132.29, 134.61, 137.34, 137.93, 139.46, 147.75, 151.57.

1-(3-(3-Chlorobenzyloxy)pyrazin-2-yl)-3-(3-fluorophenyl)urea (17)

White solid, yield: 91.5%, mp: 158.4-159.8 °C, ^{1}H NMR (400 MHz, DMSO-d_6) δ = 5.46 (2H, s, OCH2Ph), 6.86−6.88 (1H, m, ArH), 7.28-7.41 (4H, m, ArH), 7.50 (1H, d, J = 6.5 Hz, ArH), 7.58−7.61 (1H, m, ArH), 7.68 (1H, brs, ArH), 7.83 (1H, d, J = 3.0 Hz, ArH), 7.95 (1H, d, J = 3.0 Hz, ArH), 9.19 (1H, s, NH), 11.06 (1H, s, NH); ^{13}C NMR (100 MHz, $CDCl_3$) δ = 68.06, 107.62 (J_{C-F} = 26.1 Hz), 110.51 (J_{C-F} = 21.3 Hz), 115.52, 126.68, 128.80 (J_{C-F} = 16.8 Hz), 129.94, 130.06, 131.67, 132.55, 134.62, 137.27, 139.27, 139.57 (J_{C-F} = 10.6 Hz), 147.78, 151.40, 163.11 (J_{C-F} = 242.6 Hz).

1-(3-(3-Chlorobenzyloxy)pyrazin-2-yl)-3-(3-chlorophenyl)urea (18)

White solid, yield: 93.8%, mp: 151.5-152.0 °C, ^{1}H NMR (400 MHz, DMSO-d_6) δ = 5.47 (2H, s, OCH_2Ph), 7.11 (1H, dd, J = 1.1 Hz, 7.9 Hz, ArH), 7.33−7.52 (5H, m, ArH), 7.69 (1H, s, ArH), 7.82−7.83 (2H, m ArH), 7.95 (1H, d, J = 3.0 Hz, ArH), 9.19 (1H, s, NH), 11.11 (1H, s, NH); ^{13}C NMR (100 MHz, DMSO-d_6) δ = 67.35, 118.21, 119.17, 123.11, 126.98, 128.24, 128.30, 130.59, 130.90, 132.81, 133.36, 133.53, 133.73, 139.26, 139.58, 140.57, 148.97, 151.75.

1-(3-(4-Chlorobenzyloxy)pyrazin-2-yl)-3-(2,4,4-trimethylpentan-2-yl)urea (19)

White solid, yield: 70.1%, mp: 56.1-59.2 °C, HPLC purity: 8.11 min, 93.94%, ^{1}H NMR (300 MHz, DMSO-d_6) δ = 0.96 (9H, s, $3CH_3$), 1.39 (6H, s, $2CH_3$), 1.73 (2H, s, CH_2), 5.41 (2H, s, OCH_2Ph), 7.45 (2H, d, J = 8.4 Hz, ArH), 7.57 (2H, d, J = 8.4 Hz, ArH), 7.69 (1H, d, J = 3.0 Hz,

ArH), 7.78 (1H, d, *J* = 3.0 Hz, ArH), 8.12 (1H, s, NH), 8.91 (1H, s, NH). HRMS (ES^+): *m/z* calculated for $C_{20}H_{27}ClN_4O_2$: 391.1901 $[M+H]^+$. Found 391.1901.

1-(3-(4-Chlorobenzyloxy)pyrazin-2-yl)-3-(naphthalen-1-yl)urea (20)

White solid, yield: 60.8%, mp: 132.2-136.6 °C, ^1H NMR (400 MHz, DMSO-d_6 + Acetone-d_6) δ = 5.54 (2H, s, OCH_2Ph), 7.47 (2H, d, *J* = 8.4 Hz, ArH), 7.54 (1H, t, *J* = 7.9 Hz, ArH), 7.59 (1H, t, *J* = 7.2 Hz, ArH), 7.65−7.74 (4H, m, ArH), 7.87 (1H, d, *J* = 3.0 Hz, ArH), 7.99 (1H, d, *J* = 8.2 Hz, ArH), 8.08 (1H, d, *J* = 2.6 Hz, ArH), 8.18−8.25 (2H, m, ArH), 9.06 (1H, brs, NH), 11.85 (1H, brs, NH). HRMS (ES^+): *m/z* calculated for $C_{22}H_{17}ClN_4O_2$: 405.1118 $[M+H]^+$. Found 405.1117.

1-(3-(4-Fluorobenzyloxy)pyrazin-2-yl)-3-(2,4,4-trimethylpentan-2-yl)urea (21)

White solid, yield: 68.4%, mp: 110.6-111.6 °C, HPLC purity: 7.83 min, 100%, ^1H NMR (400 MHz, $CDCl_3$) δ = 1.02 (9H, s, $3CH_3$), 1.48 (6H, s, $2CH_3$), 1.80 (2H, s, CH_2), 5.37 (2H, s, OCH_2Ph), 7.07 (2H, t, *J* = 8.7 Hz, ArH), 7.14 (1H, s, NH), 7.39−7.43 (2H, m, ArH), 7.62 (2H, dd, *J* = 3.1 Hz, 16.4 Hz, ArH), 9.04 (1H, s, NH); ^{13}C NMR (100 MHz, $CDCl_3$) δ = 29.57, 31.46, 31.65, 51.64, 54.50, 67.91, 115.60 ($J_{C\text{-}F}$ = 22.1 Hz), 130.58 ($J_{C\text{-}F}$ = 9.1 Hz), 131.25, 131.38 ($J_{C\text{-}F}$ = 3.0 Hz), 131.63, 140.12, 147.63, 152.56, 162.83 ($J_{C\text{-}F}$ = 247.5 Hz). HRMS (ES^+): *m/z* calculated for $C_{20}H_{27}FN_4O_2$: 375.2196 $[M+H]^+$. Found 375.2202.

4.1.3. General procedure of chloroethyl urea derivatives 22−24

2-Chloroethyl isocyanate (0.1 mL, 1.1 mmol) was added to a solution of the appropriate 2-amino-3-benzyloxy pyrazine derivative (0.92 mmol) in dry THF (5 mL) in the presence of

DIPEA (0.5 mL, 2.75 mmol). The reaction mixture was refluxed for 18 h and evaporated after cooling. The residue was purified by flash column chromatography (SiO_2, EA/*n*-Hex = 1/4).

1-(3-(Benzyloxy)pyrazin-2-yl)-3-chloroethylurea (22)

White solid, yield: 71.3%, mp: 112.2-112.6 °C, ^{1}H NMR (400 MHz, $CDCl_3$) δ = 3.67−3.74 (4H, m, $2CH_2$), 5.41 (2H, s, OCH_2Ph), 7.36−7.43 (6H, m, ArH+NH), 7.67 (1H, d, *J* = 3.1 Hz, ArH), 7.70 (1H, d, *J* = 3.1 Hz, ArH), 9.45 (1H, s, NH); ^{13}C NMR (100 MHz, $CDCl_3$) δ = 41.93, 43.86, 68.86, 128.65, 128.71, 131.72, 132.17, 133.03, 139.60, 140.93, 154.34.

1-(3-(2-Chlorobenzyloxy)pyrazin-2-yl)-3-chloroethylurea (23)

White solid, yield: 83.4%, mp: 134.1-134.6 °C, ^{1}H NMR (400 MHz, $CDCl_3$) δ = 3.67−3.75 (4H, m, $2CH_2$), 5.52 (2H, s, OCH_2Ph), 7.27−7.35 (2H, m, ArH), 7.36 (1H, brs, NH), 7.43−7.46 (2H, m, ArH), 7.69 (1H, d, *J* = 3.1 Hz, ArH), 7.72 (1H, d, *J* = 3.1 Hz, ArH), 9.46 (1H, s, NH); ^{13}C NMR (100 MHz, $CDCl_3$) δ = 41.94, 43.87, 66.29, 127.02, 129.83, 130.04, 130.46, 131.93, 132.19, 133.11, 134.21, 139.55, 147.74, 154.29.

1-(3-(3-Chlorobenzyloxy)pyrazin-2-yl)-3-chloroethylurea (24)

White solid, yield: 84.4%, mp: 114.0-114.5 °C, ^{1}H NMR (400 MHz, $CDCl_3$) δ = 3.68−3.74 (4H, m, $2CH_2$), 5.39 (2H, s, OCH_2Ph), 7.31−7.35 (4H, m, ArH+NH), 7.41 (1H, brs, ArH), 7.67 (1H, d, *J* = 3.1 Hz, ArH), 7.72 (1H, d, *J* = 3.1 Hz, ArH), 9.44 (1H, s, NH); ^{13}C NMR (100 MHz, $CDCl_3$) δ = 41.95, 43.85, 67.88, 126.62, 128.65, 128.80, 130.02, 132.03, 132.12, 134.58, 137.40, 139.55, 147.61, 154.26

4.1.4. General procedure of piperazinethyl urea derivatives 25−28

K_2CO_3 (406.8 mg, 2.94 mmol) and the appropriate piperazine derivative (1.96 mmol) were dissolved in the solution of the appropriate chloroethyl urea derivative (1.96 mmol) in MeCN (5 mL). The reaction mixture was refluxed for 20 h and quenched by addition of water after cooling, then extracted with ethyl acetate. The organic layer was dried over anhydrous Na_2SO_4, filtered and concentrated under reduced pressure. The residue was purified by flash column chromatography (SiO_2, DCM/MeOH = 5/1).

1-(3-(Benzyloxy)pyrazin-2-yl)-3-(2-(4-methylpiperazin-1-yl)ethyl)urea (25)

White solid, yield: 45.4%, mp: 110.8-115.5 °C, ^{1}H NMR (400 MHz, $CDCl_3$) δ = 2.32 (3H, s, CH_3), 2.48−2.60 (10H, m, $5CH_2$), 3.47−3.51 (2H, m, CH_2), 5.41 (2H, s, OCH_2Ph), 7.34−7.44 (6H, m, ArH+NH), 7.65 (1H, d, *J* = 3.1 Hz, ArH), 7.69 (1H, d, *J* = 3.1 Hz, ArH), 9.31 (1H, s, NH); ^{13}C NMR (100 MHz, $CDCl_3$) δ = 37.18, 45.93, 52.61, 55.22, 56.68, 68.75, 128.60, 128.68, 131.71, 131.80, 135.46, 139.89, 147.89, 154.25.

1-(3-(2-Chlorobenzyloxy)pyrazin-2-yl)-3-(2-(4-methylpiperazin-1-yl)ethyl)urea (26)

White solid, yield: 25.1%, mp: 130.7-131.9 °C, ^{1}H NMR (300 MHz, DMSO-d_6) δ = 2.15 (3H, s, CH_3), 2.31−3.43 (10H, m, $5CH_2$), 3.31−3.34 (2H, m, CH_2), 5.50 (2H, s, OCH_2Ph), 7.37−7.40 (2H, m, ArH), 7.49−7.54 (1H, m, ArH), 7.67−7.70 (1H, m, ArH), 7.75 (1H, d, *J* = 3.0 Hz, ArH), 7.80 (1H, d, *J* = 3.0 Hz, ArH), 8.38 (1H, s, NH), 9.08 (1H, s, NH); ^{13}C NMR (100 MHz, $CDCl_3$) δ = 37.21, 46.13, 52.80, 55.40, 56.67, 66.17, 126.99, 129.79, 129.96, 130.36, 131.79, 131.95, 133.19, 134.13, 139.86, 147.68, 154.18.

1-(3-(3-Chlorobenzyloxy)pyrazin-2-yl)-3-(2-(4-methylpiperazin-1-yl)ethyl)urea (27)

White solid, yield: 27.8%, mp: 93.9-97.6 °C, HPLC purity: 4.06 min, 100%, ^{1}H NMR (400 MHz, $CDCl_3$) δ = 2.30 (3H, s, CH_3), 2.32−2.61 (8H, m, $4CH_2$), 3.33−3.51 (4H, m, $2CH_2$), 5.39 (2H, s, OCH_2Ph), 7.30−7.34 (4H, m, ArH+NH), 7.41 (1H, brs, ArH), 7.64 (1H, d, *J* = 1.0 Hz, ArH), 7.70 (1H, d, *J* = 3.1 Hz, ArH), 9.31 (1H, s, NH); ^{13}C NMR (100 MHz, $CDCl_3$) δ = 37.21, 46.14, 52.81, 54.65, 55.40, 56.66, 126.52, 128.60, 128.71, 128.76, 139.92, 131.72, 132.03, 139.89, 147.46, 154.58. HRMS (ES^+): *m/z* calculated for $C_{19}H_{25}ClN_6O_2$: 405.1806 $[M+H]^+$. Found 405.1815.

1-(3-(2-Chlorobenzyloxy)pyrazin-2-yl)-3-(2-(piperazin-1-yl)ethyl)urea (28)

White solid, yield: 29.5%, mp: 104.0-106.5 °C, HPLC purity: 3.85 min, 100%, ^{1}H NMR (300 MHz, DMSO-d_6) δ = 1.25 (s, 1H), 2.51−2.69 (12H, m, $6CH_2$), 5.50 (2H, s, OCH_2Ph), 7.37−7.40 (2H, m, ArH), 7.44 (1H, m, ArH), 7.57 (1H, m, ArH), 7.69 (1H, d, *J* = 3.0 Hz, ArH), 7.78 (1H, d, *J* = 3.0 Hz, ArH), 8.11 (1H, s, NH), 8.91 (1H, s, NH). HRMS (ES^+): *m/z* calculated for $C_{18}H_{23}ClN_6O_2$: 391.1649 $[M+H]^+$. Found 391.1640.

4.2. Biological evaluation

4.2.1. Cell culture

HT-22 (mouse hippocampal cells) cells were grown in Dulbecco's Modified Eagle's Medium (DMEM, GIBCO) supplemented with 10% (v/v) FBS and antibiotics (100 µg/mL penicillin/streptomycin mix) in a humidified atmosphere at 37 °C with 5% CO_2.

4.2.2. Protection against loss of mitochondrial membrane potential assay

HT-22 cells (30,000 per well) were seeded into a clear 96-well plate (FALCON) at 200 µL per well one day prior to assay. 750 µM of JC-1 (Stratagene) in DMSO stock solution was dissolved into phenol red-free Opti-MEM (GIBCO) medium to make final concentration of 7.5 µM JC-1 per well. Medium was removed from the plate, and 100 µL per well of JC-1 was added. Plates were incubated for 1 h and 15 min at 37 °C and washed twice with 100 µL per well PBS. Subsequently, cells were treated with 25 µL solution of each compound at 5 µM in Opti-MEM and incubated at 37 °C for 10 min followed by addition of 25 µL of Aβ (American peptide, 1–42) solution at 5 µM. Fluorescence was measured at every 1 h for 3 h at ex/em 530 nm/580 nm ('red') and ex/em 485 nm/530 nm ('green'). The ratio of green to red fluorescence was recorded and the percent changes in ratio from each compound were calculated and normalized using vehicle control as 100%.

4.2.3. Assay for cellular ATP levels (Luciferase-based assay)

10,000 HT-22 cells per well were seeded into a clear 96-well plate (FALCON) at 200 µL per well one day prior to assay. Medium was removed from the plate, and cells were treated with 25 µL solution of each compound at 10 µM and incubated at 37 °C for 10 min followed by addition of 25 µL of amyloid Beta (American peptide, 1−42) solution at 10 µM. Cells were incubated at 37 °C for 7 h and washed twice with PBS. Cells were lysed by using 1% Triton-X 100 in TBST buffer solution and protein concentrations of each well were determined via BCA protein determination kit (Thermo scientific). Equal amount of cell lysates from each well were plated into a white 96-well plate (NUNC) and the amount of ATP levels in each sample was determined by using ATP determination kit (Invitrogen). The ATP levels of each sample were subtracted with vehicle control and percent recovery were calculated based on the ATP levels of the vehicle

control treated with amyloid Beta. Assessment of compounds' effect on ATP production was based on the ATP levels of each compound treated sample without the treatment with amyloid Beta solution.

4.2.4. Cell viability MTT assay

5000 HT-22 cells per well were seeded and treated as above described method. Cells were incubated at 37 °C for 24 h. 10 µL of MTT solution (Thiazolyl blue tetrazolium bromide, Sigma) was added directly to each well and incubated at 37 °C for 2 h. After confirming the formation of blue formazan precipitates under microscope, 140 µL of solubilizing solution (10% Triton-X 100 in isopropanol with 0.1 M HCl) was added to each well followed by incubation for another hour at room temperature. Absorbance at 570 nM was measured and OD values from each well were subtracted with vehicle control and percent compounds' direct effect on viability and protective effect against amyloid Beta induced cytotoxicity were calculated by using the same method described for the ATP assay.

4.2.5. hERG K^+ channel assay

[^{3}H] Astemizole and human ERG K^+ channel expressed in HEK-293 cells were purchased from PerkinElmer. Assays were performed in 200 µL of 50 mM Hepes (pH 7.4), 60 mM KCl, 0.1% BSA, 4 nM [^{3}H] Astemizole with 2.5 µg of membranes. Assay mixtures were incubated for 1h at room temperature (RT) and filtered through a Filtermat-A pre-soaked in 0.3% PEI. The signal was detected with a MicroBeta® (PerkinElmer). Non-specific binding was determined in the presence of 0.1 µM astemizole. Competition binding studies were carried out with 5−6 varied

concentrations of the test compound run in duplicate tubes, and isotherms from two assays were calculated.

4.2.6. Molecular docking

The 3-D coordinates of human cyclophilin D-cyclosporin A complex (pdb code: 2Z6W) was downloaded from protein databank (http://www.rcsb.org). The receptor was treated with protein preparation tool applying default values as implemented in Discovery Studio 4.0 (Accelrys, San Diego, CA, USA). The binding site was defined based on contacts of cyclosporin A with cyclophilin D. Ligands were sketched as 2D structures using ChemBioDraw software then converted into minimized 3D structures by Ligand Preparation tool implemented in Discovery Studio 4.0. CDocker algorithm (Discovery Studio 4.0) was used to perform docking minimization of the ligands into the defined binding site. The retrieved docked poses were submitted to *in situ* ligand minimization within the binding pocket to calculate the binding energy and complex energy of each pose. The results were visualized and analyzed using tools implemented in Discovery Studio 4.0.

Conflict of Interest

The authors have declared no conflict of interest.

Acknowledgement

This study was supported by the KIST Institutional programs (Grant No. 2E28010) from Korea Institute of Science and Technology and by the Creative Fusion Research Program through the

Creative Allied Project funded by the National Research Council of Science & Technology (CAP-12-1-KIST).

References

[1] D.M. Holtzman, C.M. John, A. Goate, Alzheimer's Disease: The Challenge of the Second Century, Science translational medicine, 3 (2011) 77sr71-77sr71.
[2] W.W. Barker, C.A. Luis, A. Kashuba, M. Luis, D.G. Harwood, D. Loewenstein, C. Waters, P. Jimison, E. Shepherd, S. Sevush, N. Graff-Radford, D. Newland, M. Todd, B. Miller, M. Gold, K. Heilman, L. Doty, I. Goodman, B. Robinson, G. Pearl, D. Dickson, R. Duara, Relative frequencies of Alzheimer disease, Lewy body, vascular and frontotemporal dementia, and hippocampal sclerosis in the State of Florida Brain Bank, Alzheimer disease and associated disorders, 16 (2002) 203-212.
[3] M.P. Murphy, H. LeVine, Alzheimer's Disease and the β-Amyloid Peptide, Journal of Alzheimer's disease : JAD, 19 (2010) 311.
[4] W. Cerpa, M.C. Dinamarca, N.C. Inestrosa, Structure-function implications in Alzheimer's disease: effect of Abeta oligomers at central synapses, Current Alzheimer research, 5 (2008) 233-243.
[5] H. Du, L. Guo, F. Fang, D. Chen, A.A. Sosunov, G.M. McKhann, Y. Yan, C. Wang, H. Zhang, J.D. Molkentin, F.J. Gunn-Moore, J.P. Vonsattel, O. Arancio, J.X. Chen, S.D. Yan, Cyclophilin D deficiency attenuates mitochondrial and neuronal perturbation and ameliorates learning and memory in Alzheimer's disease, Nature medicine, 14 (2008) 1097-1105.
[6] P.H. Reddy, M.F. Beal, Amyloid beta, mitochondrial dysfunction and synaptic damage: implications for cognitive decline in aging and Alzheimer's disease, Trends in molecular medicine, 14 (2008) 45-53.
[7] G. Morciano, C. Giorgi, M. Bonora, S. Punzetti, R. Pavasini, M.R. Wieckowski, G. Campo, P. Pinton, Molecular identity of the mitochondrial permeability transition pore and its role in ischemia-reperfusion injury, Journal of Molecular and Cellular Cardiology, 78 (2015) 142-153.
[8] J. Karch, J.D. Molkentin, Identifying the components of the elusive mitochondrial permeability transition pore, Proceedings of the National Academy of Sciences of the United States of America, 111 (2014) 10396-10397.
[9] A.A. Starkov, F.M. Beal, Portal to Alzheimer's disease, Nature medicine, 14 (2008) 1020-1021.
[10] P. Bernardi, Mitochondrial transport of cations: channels, exchangers, and permeability transition, Physiological reviews, 79 (1999) 1127-1155.
[11] H.X. Guo, F. Wang, K.Q. Yu, J. Chen, D.L. Bai, K.X. Chen, X. Shen, H.L. Jiang, Novel cyclophilin D inhibitors derived from quinoxaline exhibit highly inhibitory activity against rat mitochondrial swelling and Ca2+ uptake/ release, Acta pharmacologica Sinica, 26 (2005) 1201-1211.
[12] S. Murasawa, K. Iuchi, S. Sato, T. Noguchi-Yachide, M. Sodeoka, T. Yokomatsu, K. Dodo, Y. Hashimoto, H. Aoyama, Small-molecular inhibitors of Ca(2)(+)-induced mitochondrial permeability transition (MPT) derived from muscle relaxant dantrolene, Bioorganic & medicinal chemistry, 20 (2012) 6384-6393.
[13] S. Roy, J. Sileikyte, M. Schiavone, B. Neuenswander, F. Argenton, J. Aube, M.P. Hedrick, T.D. Chung, M.A. Forte, P. Bernardi, F.J. Schoenen, Discovery, Synthesis, and Optimization of Diarylisoxazole-3-carboxamides as Potent Inhibitors of the Mitochondrial Permeability Transition Pore, ChemMedChem, 10 (2015) 1655-1671.

[14] S. Roy, J. Sileikyte, B. Neuenswander, M.P. Hedrick, T.D. Chung, J. Aube, F.J. Schoenen, M.A. Forte, P. Bernardi, N-Phenylbenzamides as Potent Inhibitors of the Mitochondrial Permeability Transition Pore, ChemMedChem, 11 (2016) 283-288.
[15] S. Ni, Y. Yuan, J. Huang, X. Mao, M. Lv, J. Zhu, X. Shen, J. Pei, L. Lai, H. Jiang, J. Li, Discovering potent small molecule inhibitors of cyclophilin A using de novo drug design approach, Journal of medicinal chemistry, 52 (2009) 5295-5298.
[16] J. Kim, J. Lee, B. Moon, I. Mook-Jung, G. Nam, G. Keum, A.N. Pae, H. Choo, Pyridyl-urea Derivatives as Blockers of Aβ-induced mPTP Opening for Alzheimer's Disease, Bulletin of the Korean Chemical Society, 33 (2012) 3887-3888.
[17] Y.S. Kim, S.H. Jung, B.G. Park, M.K. Ko, H.S. Jang, K. Choi, J.H. Baik, J. Lee, J.K. Lee, A.N. Pae, Y.S. Cho, S.J. Min, Synthesis and evaluation of oxime derivatives as modulators for amyloid beta-induced mitochondrial dysfunction, European journal of medicinal chemistry, 62 (2013) 71-83.
[18] A. Elkamhawy, J.E. Park, A.H.E. Hassan, A.N. Pae, J. Lee, B.G. Park, E.J. Roh, Synthesis and evaluation of 2-(3-arylureido)pyridines and 2-(3-arylureido)pyrazines as potential modulators of Abeta-induced mitochondrial dysfunction in Alzheimer's disease, European journal of medicinal chemistry, 144 (2018) 529-543.
[19] A. Elkamhawy, J.E. Park, A.H.E. Hassan, H. Ra, A.N. Pae, J. Lee, B.G. Park, B. Moon, H.M. Park, E.J. Roh, Discovery of 1-(3-(benzyloxy)pyridin-2-yl)-3-(2-(piperazin-1-yl)ethyl)urea: A new modulator for amyloid beta-induced mitochondrial dysfunction, European journal of medicinal chemistry, 128 (2017) 56-69.
[20] A. Elkamhawy, J. Lee, B.G. Park, I. Park, A.N. Pae, E.J. Roh, Novel quinazoline-urea analogues as modulators for Abeta-induced mitochondrial dysfunction: design, synthesis, and molecular docking study, European journal of medicinal chemistry, 84 (2014) 466-475.
[21] S. Jung, K. Choi, A.N. Pae, J.K. Lee, H. Choo, G. Keum, Y.S. Cho, S.J. Min, Facile diverted synthesis of pyrrolidinyl triazoles using organotrifluoroborate: discovery of potential mPTP blockers, Organic & biomolecular chemistry, 12 (2014) 9674-9682.
[22] J.E. Park, A. Elkamhawy, A.H.E. Hassan, A.N. Pae, J. Lee, S. Paik, B.G. Park, E.J. Roh, Synthesis and evaluation of new pyridyl/pyrazinyl thiourea derivatives: Neuroprotection against amyloid-beta-induced toxicity, European journal of medicinal chemistry, 141 (2017) 322-334.
[23] S.T. Smiley, M. Reers, C. Mottola-Hartshorn, M. Lin, A. Chen, T.W. Smith, G.D. Steele, L.B. Chen, Intracellular heterogeneity in mitochondrial membrane potentials revealed by a J-aggregate-forming lipophilic cation JC-1, Proceedings of the National Academy of Sciences, 88 (1991) 3671.
[24] M. Reers, T.W. Smith, L.B. Chen, J-aggregate formation of a carbocyanine as a quantitative fluorescent indicator of membrane potential, Biochemistry, 30 (1991) 4480-4486.
[25] R.C. Reid, M.K. Yau, R. Singh, J. Lim, D.P. Fairlie, Stereoelectronic effects dictate molecular conformation and biological function of heterocyclic amides, Journal of the American Chemical Society, 136 (2014) 11914-11917.
[26] A. Elkamhawy, J.E. Park, A.H.E. Hassan, A.N. Pae, J. Lee, B.G. Park, S. Paik, J. Do, J.H. Park, K.D. Park, B. Moon, W.K. Park, H. Cho, D.Y. Jeong, E.J. Roh, Design, synthesis, biological evaluation and molecular modelling of 2-(2-aryloxyphenyl)-1,4-dihydroisoquinolin-3(2H)-ones: A novel class of TSPO ligands modulating amyloid-beta-induced mPTP opening, European journal of pharmaceutical sciences : official journal of the European Federation for Pharmaceutical Sciences, 104 (2017) 366-381.
[27] E.A.G. Blomme, Y. Will, Toxicology Strategies for Drug Discovery: Present and Future, Chemical Research in Toxicology, 29 (2016) 473-504.
[28] K. Chan, D. Truong, N. Shangari, P.J. O'Brien, Drug-induced mitochondrial toxicity, Expert Opinion on Drug Metabolism & Toxicology, 1 (2005) 655-669.
[29] C. Jamieson, E.M. Moir, Z. Rankovic, G. Wishart, Medicinal chemistry of hERG optimizations: Highlights and hang-ups, Journal of medicinal chemistry, 49 (2006) 5029-5046.

[30] A.A. Lagrutta, E.S. Trepakova, J.J. Salata, The hERG channel and risk of drug-acquired cardiac arrhythmia: an overview, Current topics in medicinal chemistry, 8 (2008) 1102-1112.
[31] K. Kajitani, M. Fujihashi, Y. Kobayashi, S. Shimizu, Y. Tsujimoto, K. Miki, Crystal structure of human cyclophilin D in complex with its inhibitor, cyclosporin A at 0.96-A resolution, Proteins, 70 (2008) 1635-1639.

Highlights

- Biological activity of 17 analogs against Aβ-induced mPTP opening was superior to that of CsA.
- Derivative **5** had a safe profile regarding ATP production, cell viability and hERG.
- Molecular modeling study predicted plausible binding modes explaining the elicited mPTP blocking activity.
- This study suggests compound **5** as potential lead for further development towards AD therapy.